Mon. Not. R. Astron. Soc. **000**, 000–000 (0000) Printed 22 January 2009 (MN LATEX style file v2.2)

Neutrino Masses, Dark Energy and the Gravitational Lensing of Pregalactic HI

R. Benton Metcalf
Max Plank Institut für Astrophysics, Karl-Schwarzchild-Str. 1, 85741 Garching, Germany

22 January 2009

ABSTRACT

We study the constraints which the next generation of radio telescopes could place on the mass and number of neutrino species by studying the gravitational lensing of high redshift 21 cm emission in combination with wide-angle surveys of galaxy lensing. We use simple characterizations of reionization history and of proposed telescope designs to forecast the constraints and detectability threshold for neutrinos. It is found that the degeneracy between neutrino parameters and dark energy parameters is significantly reduced by incorporating 21 cm lensing. The combination of galaxy and 21 cm lensing could constrain the sum of the neutrino masses to within ~ 0.04 eV and the number of species to within ~ 0.1. This is an improvement of a factor of 2.6 in mass and 1.3 in number over a galaxy lensing survey alone. This includes marginalizing over an 11 parameter cosmological model with a two parameter model for the dark energy equation of state. If the dark energy equation of state is held fixed at $w \equiv p/\rho = -1$ the constraints improve to ~ 0.03 eV and 0.04. These forecasted errors depend critically on the fraction of sky that can be surveyed in redshifted 21 cm emission (25% is assumed here) and the redshift of reionization ($z = 7$ is assumed here). It is also found that neutrinos with masses too small to be detected in the data could none the less cause a significant bias in the measured dark energy equation of state.

Key words: large-scale structure of Universe – dark matter – gravitational lensing – intergalactic medium – low frequency radio astronomy

1 INTRODUCTION

One of the most tantalizing questions in experimental particle physics – the nature of neutrino mass – is connected to one of the most tantalizing questions in observational cosmology – the nature of dark energy. Cosmological observations presently put the most stringent upper limits on the absolute mass of neutrinos (Seljak et al. 2005; Spergel et al. 2007) and might continue to do so for some time to come. However, a partial degeneracy between neutrino masses and the dark energy's equation of state limits how well either one can be determined from cosmological measurements based on the evolution of structure formation.

Atmospheric and solar neutrino oscillation experiments strongly indicate that neutrinos have mass and that the sum of their masses is larger than the measured mass splittings $\sum_\nu m_\nu \gtrsim \sqrt{\Delta m^2_{\rm atm}} + \sqrt{\Delta m^2_{\rm sun}} \simeq 0.05$ eV. Direct measurements from β-decay experiments give an upper bound on the electron neutrino mass of 2.5 eV, there are no competing measurements of the other flavors (see Fogli et al. (2006) for a review of experimental results). Combinations of cosmological data give a constraint of $\sum_\nu m_\nu < 0.66$ eV assuming a flat cosmology with a cosmological constant, but this limit is considerably looser if the density of dark energy is allowed to evolve with time (Seljak et al. 2005; Hannestad 2005; Spergel et al. 2007).

Massive neutrinos in the appropriate mass range are relativistic when they decouple from the photons, electrons and baryons when the temperature of the universe is a few MeV. They have the effect of suppressing the power spectrum of density fluctuations on small scales (scales smaller than the horizon when the neutrinos become non-relativistic, $k > k_{\rm nr} \simeq 0.018\sqrt{m_\nu \Omega_m}\ h$ Mpc^{-1} eV$^{-1/2}$ where k is the Fourier wave number, m_ν is the neutrino's mass and h is the Hubble parameter in units of 100 km s^{-1}Mpc^{-1}) due to free-steaming. This suppression begins at the time of decoupling and continues until today because the thermal velocity of the neutrinos is still significant ($v_{\rm therm} \simeq 150\ (1+z)\ m_\nu$ km s^{-1}eV^{-1} when non-relativistic). The free-streaming scale continues to decrease from its maximum of $k_{\rm nr}$ as $k_{\rm fs} \simeq 0.82 \frac{\sqrt{\Omega_m (1+z)^3 + \Omega_\Lambda}}{(1+z)^2} \left(\frac{m_\nu}{\rm eV}\right) h$ Mpc^{-1}. Neutrinos will resist falling into dark matter halos with velocity dispersions $\lesssim v_{\rm therm}$. For a review of neutrinos in cosmology see Lesgourgues & Pastor (2006).

It has been proposed that neutrino masses could be

measured by the next generation of weak gravitational lensing surveys (EUCLID[1],LSST[2],PanSTARRS[3], DES[4]) (Hannestad et al. 2006; Kitching et al. 2008) and that the existence of massive neutrinos may limit the ability of these surveys to measure properties of the dark energy (Hannestad 2005; Kiakotou et al. 2007). Dark energy causes structure formation to evolve differently than it would otherwise at low redshift ($z \lesssim 1$). A degeneracy arises between this and the late-time free-streaming of massive neutrinos since at scales significantly smaller than $k_{\rm fs}$ the suppression is scale independent and the lensing surveys will be sensitive to a limited range in k. However, at $z > 1$ dark energy is expected to have negligible effects on structure formation so if higher redshifts can be probed the degeneracy can be removed. The CMB (cosmic microwave background) provides information on the power spectrum at $z \sim 1100$, but Silk damping limits its sensitivity to scales below $k_{\rm nr}$. Gravitational lensing of pregalactic 21-cm radiation can provide a probe of structure formation on the scales needed, at the redshifts needed.

The prospects for measuring gravitational lensing of the pregalactic 21 cm radiation have been studied by a number of authors (Zahn & Zaldarriaga 2006; Metcalf & White 2007b; Hilbert et al. 2007; Lu & Pen 2007; Metcalf & White 2007a). The methods used in this paper are described in more detail in Metcalf & White (2007a).

2 FORMALISM & MODELING

2.1 pregalactic 21 cm radiation

A thorough review of pregalactic 21 cm radiation can be found in Furlanetto et al. (2006). For this paper we will mention only the barest essentials needed to specify our model for 21 cm emission. The fluctuations in the 21 cm brightness temperature depend on the spin temperature, T_s, the ionization fraction, $x_{\rm H}$ and the density of HI through

$$\delta T_b \simeq 24(1+\delta_b)x_{\rm H}\left(\frac{T_s - T_{\rm CMB}}{T_s}\right)\left(\frac{\Omega_b h^2}{0.02}\right) \times \left(\frac{0.15}{\Omega_m h^2}\frac{1+z}{10}\right)^{1/2} \ {\rm mK} \qquad (1)$$

(Field 1959; Madau et al. 1997). As is commonly done, we will assume that the spin temperature is much greater than the CMB temperature. This leaves fluctuations in x_H, and the baryon density $\delta_b = (\rho_b - \overline{\rho}_b)/\overline{\rho}_b$ as the sources of brightness fluctuations. We will make the simplifying assumption that $x_{\rm H} = 1$ until the universe is very rapidly and uniformly reionized at a redshift of $z_{\rm reion}$. We will take δ_b to be distributed in the same way as dark matter according to the CDM model. Nonlinear structure formation (Peacock & Dodds 1996) and linear redshift distortion (Kaiser 1987) are included. Realistically, the reionization process will be inhomogeneous and may extend over a significant redshift range. This will increase $C_\nu(\ell)$ by perhaps a factor of 10 on scales larger than characteristic size of the ionized bubbles (Zaldarriaga et al. 2004) and make the distribution non-Gaussian.

2.2 gravitational lensing

It is convenient to express the lensing formalism in terms of the convergence, $\kappa(\vec{\theta}, z_s)$, at a position $\vec{\theta}$ on the sky which to an excellent approximation is related directly to the distribution of matter through which the light passes

$$\kappa\left(\vec{\theta}, z_s\right) = \frac{3}{4}H_o\Omega_m\int_0^\infty dz\ \frac{(1+z)}{E(z)}g\left(z, z_s\right)\delta\left(\vec{\theta}, z\right) \qquad (2)$$

$$\simeq \frac{3}{4}H_o\Omega_m\sum_i \delta\left(\vec{\theta}, z_i\right)\int_{z_i-\delta z}^{z_i+\delta z} dz\ \frac{(1+z)}{E(z)}g\left(z, z_s\right)$$

$$= \sum_i G(z_i, z_s)\delta\left(\vec{\theta}, z_i\right) \qquad (3)$$

with

$$g(z, z_s) = \int_z^\infty dz'\ \eta\left(z', z_s\right)\frac{D(z,0)D(z',z)}{D(z',0)}. \qquad (4)$$

H_o is the Hubble parameter. The convergence can be thought of as a projected dimensionless surface density. The weighting function for the source distance distribution, $\eta(z)$, is normalized to unity. $D(z', z)$ is the angular size distance between the two redshifts and $\delta(\vec{x}, z)$ is the fractional density fluctuation at redshift z and perpendicular position $\vec{x}$. The function

$$E(z) = \sqrt{\Omega_m(1+z)^3 + \Omega_\Lambda(1+z)^{3f(z)}}, \qquad (5)$$

where Ω_m and Ω_Λ, are the present day densities of matter and dark energy measured in units of the critical density. It is assumed that the universe is flat – $\Omega_m + \Omega_\Lambda = 1$. The function describing the evolution of dark energy with redshift can be written

$$f(z) = \frac{-1}{\ln(1+z)}\int_{-\ln(1+z)}^0 [1 + w(a)]\ d\ln a \qquad (6)$$

where $w(a)$ is the equation of state parameter for the dark energy – the ratio of the of its pressure to its density – and $a = (1+z)^{-1}$ is the scale parameter.

For our purposes it is convenient to express equation (3) as a matrix equation,

$$\mathbf{K} = \mathbf{G}\boldsymbol{\delta}, \qquad (7)$$

where the the components of $\mathbf{K}$ are the convergences running over all position angles $\vec{\theta}$ and source redshifts, z_s. The components of the vector $\boldsymbol{\delta}$ run over all position angles and foreground redshifts z_i. The matrix $\mathbf{G}$ is a function of most of the global cosmological parameters – Ω_m, Ω_Λ, w, etc – and is independent of position on the sky. This equation holds equally well if κ and δ are expressed spherical harmonic space or in the u-v plane where interferometer observations are carried out.

Within frequency bands of size 1 MHz we use an estimator for the Fourier transform of the convergence, $\kappa(\ell, z_s)$, denoted $\hat{\kappa}(\ell, z_s)$, based on the Zahn & Zaldarriaga (2006) estimator and then combine the bands as in Metcalf & White

[1] www.dune-mission.net
[2] www.lsst.org
[3] pan-stars.ifa.hawaii.edu
[4] https://www.darkenergysurvey.org/

(2007a). The noise in $\hat{\kappa}(\ell,\nu)$ within one frequency band is

$$N^{\hat{\kappa}}(\ell,\nu) = \frac{(2\pi)^2}{2} \times \left[\sum_k \int d^2\ell' \, \frac{[\boldsymbol{\ell}\cdot\boldsymbol{\ell}'\, C_\nu(\ell',k) + \boldsymbol{\ell}\cdot(\boldsymbol{\ell}-\boldsymbol{\ell}')\, C_\nu(|\boldsymbol{\ell}'-\boldsymbol{\ell}|,k)]^2}{C_\nu^T(\ell',k) C_\nu^T(|\boldsymbol{\ell}'-\boldsymbol{\ell}|,k)}\right]^{-1} \quad (8)$$

where $C_\nu^T(\ell,k)$ is the power spectrum of the actual brightness temperature, while $C_\nu(\ell,k) = C_\nu^T(\ell,k) + C_\nu^N(\ell,k)$ is the observed power spectrum which includes noise. ℓ is the angular Fourier mode number. Because the estimator is a sum over all the observed pairs of visibilities, it will (by the central limit theorem) be close to Gaussian distributed even though it is quadratic in the visibilities.

The $\hat{\kappa}(\ell,z)$s can be grouped into a data vector

$$\mathbf{D} = \hat{\mathbf{K}} - \mathbf{K} \quad (9)$$

$$= \hat{\mathbf{K}} - \mathbf{G}\boldsymbol{\delta} \quad (10)$$

where the components run over all the combinations of z_i and ℓ that are measured. To a good approximation modes from different bands and ℓ's separated by more than the resolution of the telescope are statistically independent so the covariance matrix for $\mathbf{D}$ is diagonal

$$\mathbf{N}_{ij} \simeq \delta_{ij} N^{\hat{\kappa}}(\ell_i,\nu_i). \quad (11)$$

with $|\ell_i - \ell_j|$ larger than the resolution. The likelihood function for the correlations in $\kappa(\ell,z_i)$ is given by

$$\ln\mathcal{L} = -\frac{1}{2}\hat{\mathbf{K}}^\dagger \mathbf{C}^{-1}\hat{\mathbf{K}} - \frac{1}{2}|\mathbf{C}|, \quad (12)$$

where

$$\mathbf{C} = \mathbf{N} + \mathbf{C}_\kappa \quad (13)$$

(Metcalf & White 2007a). $\mathbf{C}_\kappa$ here is the (cross-)power spectrum of the convergence for two different source redshifts,

$$[\mathbf{C}_\kappa]_{ij} = \left\langle \kappa(\vec{\ell},z_i)\kappa(\vec{\ell},z_j)\right\rangle. \quad (14)$$

This can be calculated using expression (2) and a model for the matter power spectrum.

2.3 structure formation with massive neutrinos

To calculate the linear matter power spectrum we use the analytic formulae of Eisenstein & Hu (1999) with the modification of Kiakotou et al. (2007) that improves accuracy when the neutrino masses are small. We use the method of Peacock & Dodds (1996) to transform this linear power spectrum into a power spectrum with nonlinear structure formation. This method has not been tested thoroughly against simulations of nonlinear structure formation with massive neutrinos, but we expect that the relation between the linear and nonlinear power spectrum will be only weakly affected by this. There is no baryon acoustic oscillations in the power spectrum.

We assume that there are N_ν species of neutrinos with the same mass. The total density of neutrinos is fixed by the physics at the time of decoupling to be $\Omega_\nu h^2 = \sum_\nu m_\nu/93.14$ eV. If the masses are not degenerate the measured N_ν will not be an integer. These are the parameters we will try to constrain. Roughly speaking N_ν controls the average mass of the neutrino species and through this the free-streaming scale while $\Omega_\nu h^2$ affects the degree of suppression to the power spectrum.

The measurements we consider are actually sensitive to any light particle species with significant cosmological densities not just neutrinos. The interpretation of the parameters would be different for relic particles that were produced in a different way, for example axions, but the late-time physics would be the same.

2.4 model observations

2.4.1 21 cm observations

We will concentrate on the planned SKA (the Square Kilometer Array)[5] because it is the only planned telescope that will have a large enough size to be relevant to neutrino constraints. It is only the core of the telescope that will be used for observing pregalactic 21 cm radiation. Plans for the SKA core have not been finalized, but it is expected to have a diameter of $D_{\rm tel} \sim 6$ km ($\ell_{\rm max} \sim 10^4$), an aperture covering fraction of $f_{\rm cover} \sim 0.02$ (the total collecting area of the telescopes divided by $\pi(D_{\rm tel}/2)^2$) and a frequency range extending down to ~ 100 MHz which corresponds to $z \sim 13$. It is expected that the SKA will be able to map the 21 cm emission with a resolution of $\Delta\theta \sim 1$ arcmin. For reference, one arcminute (fwhm) corresponds to baselines of 5.8 km at $z = 7$ and 11 km at $z = 15$. We will take $\ell_{\rm min} = 10$ to be the lowest mode to be measured.

The noise in each visibility measurement will have a thermal component and a component resulting from imperfect foreground subtraction. Here we model only the thermal component. If the telescopes in the array are uniformly distributed on the ground, the average integration time for each baseline will be the same and the power spectrum of the noise will be

$$C_\ell^N = \frac{2\pi}{\Delta\nu t_o}\left(\frac{T_{\rm sys}\lambda}{f_{\rm cover} D_{\rm tel}}\right)^2 = \frac{(2\pi)^3 T_{\rm sys}^2}{\Delta\nu t_o f_{\rm cover}^2 \ell_{\rm max}(\nu)^2}, \quad (15)$$

(Zaldarriaga et al. 2004; Morales 2005; McQuinn et al. 2006) where $T_{\rm sys}$ is the system temperature, $\Delta\nu$ is the bandwidth, t_o is the total observation time, and $\ell_{\rm max}(\lambda) = 2\pi D_{\rm tel}/\lambda$ is the highest multipole that can be measured by the array, as set by the largest baselines. At the relevant frequencies, the overall system temperature is expected to be dominated by galactic synchrotron radiation. We will approximate the brightness temperature of this foreground as $T_{\rm sky} = 180\ {\rm K}(\nu/180\ {\rm MHz})^{-2.6}$, as appropriate for regions well away from the Galactic Plane (Furlanetto et al. 2006). This results in larger effective noise for higher redshift measurements of the 21 cm emission. We will consider an observation time of 90 days which might be achievable within three seasons of observation and we will assume that the survey covers 25% of the sky.

2.4.2 galaxy weak lensing survey

For comparison and for combining with the 21 cm lensing we will consider a model galaxy lensing survey. The noise in

[5] www.skatelescope.org/

power spectrum estimates from such a survey can be written as $N_\kappa(\ell) = \sigma_\epsilon^2/n_{\rm g}$ where $n_{\rm g}$ is the angular number density of background galaxies and σ_ϵ is the root-mean-square intrinsic ellipticity of those galaxies. This neglects all systematic errors as well as photometric redshift uncertainties. Following standard assumptions, we model the redshift distribution of usable galaxies as $\eta(z) \propto z^2 e^{-(z/z_o)^{1.5}}$, where z_o is set by the desired median redshift, and we adopt $\sigma_\epsilon = 0.25$. The EUCLID satellite (the imaging part of which was previously known as DUNE[6]) proposes to survey 20,000 square degrees on the sky to a usable galaxy density of $n_{\rm g} \simeq 35$ arcmin^{-2} with a median redshift of $z \sim 0.9$. Several planned ground-based surveys – LSST, PanSTARRS – will cover comparable areas to EUCLID at a similar depth. In order to use tomographic information, we divide the galaxies into 10 redshift bins each containing the same number of galaxies.

2.4.3 CMB observations

The Planck Surveyor[7] will do a full sky survey of the CMB radiation with higher resolution and more sensitivity to polarization than is now available. We incorporate these future measurements into our forecasts by calculating the expected Fisher matrix. To do this we use the same technique as described in the appendix of Rassat et al. (2008). This includes the contributions from both the scalar and tensor perturbations.

2.5 the cosmology

We use a 11 parameter cosmological model. The energy densities in dark energy and baryons are Ω_Λ and Ω_b in units of the critical density. The density of matter is fixed to $\Omega_m = 1 - \Omega_\Lambda$ to make the geometry flat. The primordial power spectrum is

$$P_o(k) = A_s \left(\frac{k}{H_o c^{-1}}\right)^{n_s + \frac{dn_s}{d\ln k}\ln k} \qquad (16)$$

The $\frac{dn_s}{d\ln k}$ parameter is included because if the primordial power spectrum is not a pure power-law it might partially mock the effect of early neutrino free-streaming on the power spectrum. The time dependent dark energy equation of state has two parameters $w(a) = w_o + w_a(1-a)$. There are two neutrino parameter N_ν and $\sum_\nu m_\nu$. Including $\frac{dn_s}{d\ln k}$ and a non-constant w makes this a more general set of parameters with more potential degeneracies than has usually been used when predicting constraints on massive neutrinos. The optical depth to CMB last scattering surface is τ. The fiducial model is set to $\{\tau, h, \Omega_\Lambda h^2, \Omega_b h^2, n_s, \frac{dn_s}{d\ln k}, w_o, w_a, N_\nu\} = \{0.09, 0.7, 0.343, 0.0223, 1, 0, -1, 0, 3\}$. The normalization, A_s, is set so that the fluctuations within a sphere of radius 8 Mpc is $\sigma_8 = 0.75$ in the fiducial model. Two values for $\Sigma_\nu m_\nu$ are used, 0.66 eV and 0.09 eV. All calculated parameter constraints are marginalized over the other parameters.

[6] www.dune-mission.net
[7] www.rssd.esa.int/index.php?project=Planck

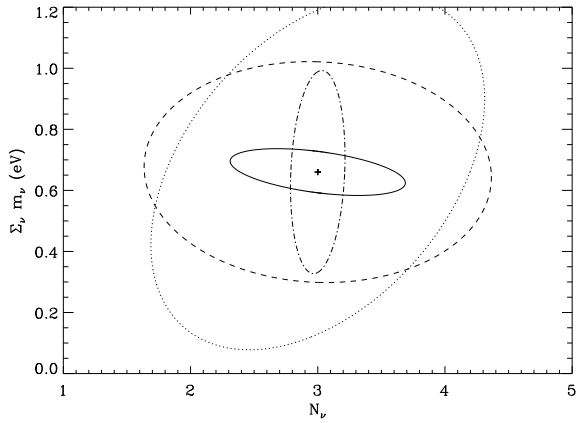

Figure 1. The forecasted constraints on the combined mass and number of neutrinos with the fiducial model $\{\sum_\nu m_\nu, N_\nu\} = \{0.66\text{ eV}, 3\}$ marginalized over all the other cosmological parameters. The dotted curves are for a EUCLID-like galaxy lensing survey, the dashed curves are for a 21 cm lensing survey, the solid curves are for the tomographic combination of the two surveys and the dot-dashed curve is for Planck by itself.

3 RESULTS

To assess how well the proposed observations could measure neutrino properties we adopt two statistical methods that are popular in the literature – Fisher matrix forecasts and the Bayesian evidence method.

3.1 Fisher matrix forecast

The maximum likelihood estimate for any parameter can be found by maximizing (12) with respect to that parameter. The error in this estimator is often forecast using the Fisher matrix defined as

$$\mathbf{F}_{ij} = -\left\langle \frac{\partial^2 \ln \mathcal{L}}{\partial p_i \partial p_j} \right\rangle . \qquad (17)$$

The expected error in the parameter p_a, marginalized over all other parameters, is $\sigma_a^2 \simeq \left(\mathbf{F}^{-1}\right)_{aa}$. The unmarginalized error estimate (the error when all other parameters are held fixed) is $\left(\mathbf{F}_{aa}\right)^{-1}$.

Since ℓ-modes separated by more than the resolution of the telescope will not be correlated, we can break the likelihood function up into factors representing each resolved region in ℓ-space (Metcalf & White 2007b). The result is that there are $\sim (2\ell+1) f_{\rm sky}$ independent measured modes for each value of ℓ, where $f_{\rm sky}$ is the fraction of sky surveyed. The Fisher matrix can then be further simplified to the widely used form,

$$\mathbf{F}_{ab} = \frac{1}{2}\sum_{\ell=\ell_{\rm min}}^{\ell_{\rm max}} (2\ell+1) f_{\rm sky} {\rm tr}\left[\mathbf{C}^{-1}\mathbf{C}_{,a}\,\mathbf{C}^{-1}\mathbf{C}_{,b}\right] . \qquad (18)$$

The error estimates on the neutrino parameters are shown in figures 1 through 3 for combinations of different data and model assumptions. Figure 1 shows the constraints using the three kinds of data by themselves and the combination of galaxy and 21 cm lensing. These lensing surveys are combined tomographically not just by adding their Fisher

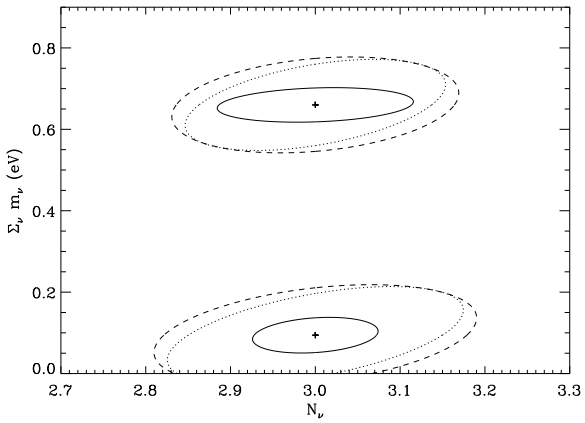

Figure 2. The same as figure 1 except the Planck constraints are combined with the lensing constraints and the scale has been changed. There are two fiducial models at $\{\sum_\nu m_\nu, N_\nu\} = \{0.66\text{ eV}, 3\}$ and $\{\sum_\nu m_\nu, N_\nu\} = \{0.09\text{ eV}, 3\}$.

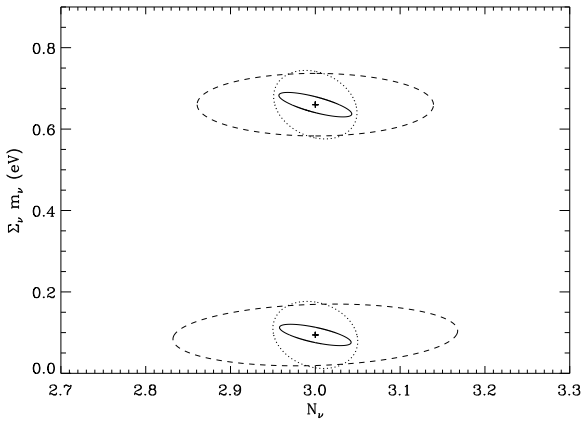

Figure 3. Same as figure 2 except the dark matter equation of state is held fixed at $\{w_o, w_a\} = \{-1, 0\}$.

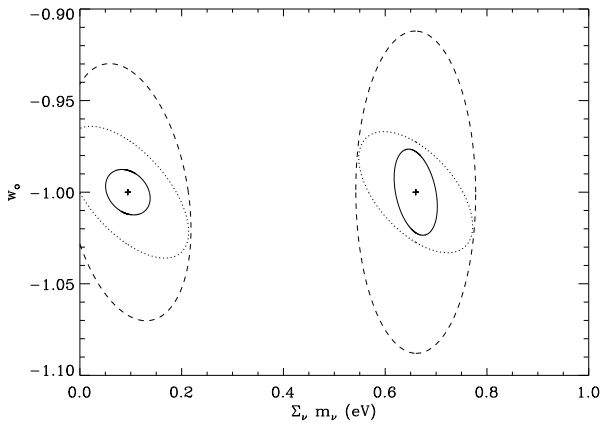

Figure 4. The constraints in the $w_o - \sum_\nu m_\nu$ plane. Planck constraints are included. Note the improvement in the w_a constraints especially when the neutrino masses are small.

matrices as would be the case if they were independent measurements. Ten redshift bins with equal numbers of galaxies are used and ten redshift bins of fixed z-width are used for the 21 cm lensing. The CMB does a relatively good job of constraining the N_ν, but not as good a job of constraining the sum of the masses.

In figure 2 the CMB constraints are combined with the lensing constraints. There is a drastic improvement because the parameter degeneracies are significantly reduced (Note the change in scale from figure 1). The forecasted errors are 0.04 eV and 0.1 for the combination of lensing surveys with $\sum_\nu m_\nu = 0.66$. This is an improvement of 2.6 in mass and 1.3 in N_ν over either of the lensing surveys by themselves. In figure 3 the dark energy equation of state is kept fixed ($w = -1$). The improvement in the constraints illustrates the degeneracy between neutrinos and dark energy parameters. The effect on the galaxy lensing constraints are particularly strong. If one only considers cosmological constant models the constraints improve to 0.03 eV and 0.04 for the combined lensing case.

Figure 4 shows the constraints in the w_o - $\sum_\nu m_\nu$ plane. It can be seen more directly here how the degeneracy between dark energy and massive neutrinos is reduced by including 21 cm lensing, especially when the neutrino masses are small. Note also that if it were assumed that neutrinos are massless, the maximum likelihood would not give the correct value for w_o.

These calculations are in agreement with previous calculations of the constraints from future galaxy lensing surveys (Kitching et al. 2008; Hannestad et al. 2006) where more restricted cosmological models were used and thus stronger constraints were found.

3.2 Bayesian evidence

Another statistical question that could be asked is whether the data *requires* massive neutrinos. One way to answer this question is using the average ratio of the Bayesian evidence (Jeffreys 1961) for models with and without massive neutrinos. This technique has been used extensively in cosmological parameter estimation (Liddle et al. (2006); Saini et al. (2004); Heavens et al. (2007) for example) and galaxy lensing surveys specifically (Kitching et al. 2008).

The Bayesian evidence is the probability of the data, D, given the model, M, marginalized over the parameters of that model, $\{\theta\}$,

$$E(D|M) = \int d\theta\ p(D|\theta, M)p(\theta|M). \tag{19}$$

The integral is over all of the parameter space. Bayes factor is the ratio of the evidences for two competing models

$$B \equiv \frac{E(D|M_o)}{E(D|M_1)}. \tag{20}$$

Here model M_o is the simpler model with n_o parameters and model M_1 is more complex and has more parameters, $n_1 > n_o$.

To make a forecast, Bayes factor must be averaged over expected data sets. It will be assumed that model M_o is the real case so that the averaging is according to this model. We are asking how well we can expect to role out model M_1.

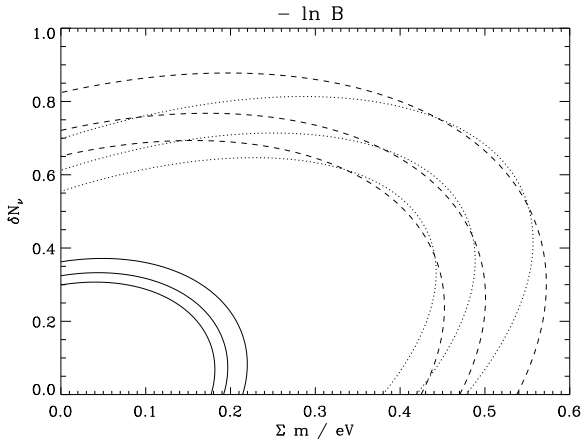

Figure 5. The log of the average evidence ratio between a model with and without massive neutrinos. The axis are the deviation from the fiducial model $\{\sum_\nu m_\nu, N_\nu\} = \{0, 3\}$. The three contour curves of each type are for 1, 2.5 and 5. According to Jeffreys (1961) $|\ln B| < 1$ is "inconclusive", $1 < |\ln B| < 2.5$ is "substantial", $2.5 < |\ln B| < 5$ is "strong" and $|\ln B| > 5$ is "decisive" evidence for the additional parameters. The expected constraints from Planck have been incorporated. The dotted curves are for a EUCLID-like galaxy lensing survey, the dashed curves are for a 21 cm lensing survey and the solid curves are for the tomographic combination of the two surveys.

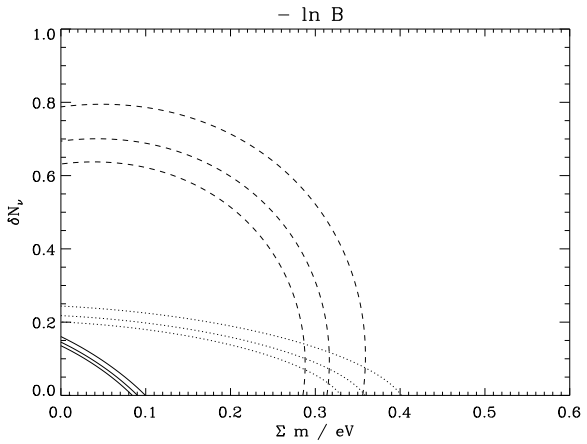

Figure 6. Same as figure 5 except the dark matter equation of state is held fixed at $\{w_o, w_a\} = \{-1, 0\}$.

In calculating this we use the approximation to $\langle B\rangle$ derived by Heavens et al. (2007) the Savage-Dickey ratio

$$\langle B\rangle \simeq (2\pi)^{-(n_1-n_o)/2}\sqrt{\frac{|F^{(1)}|}{|F^{(o)}|}}\exp\left[-\frac{1}{2}\delta\theta_\nu F^{(1)}_{\nu\mu}\delta\theta_\mu\right] \quad (21)$$

where

$$\delta\theta_i = \left[\left(F^{(o)}\right)^{-1}\right]_{ij} F^{(1)}_{j\alpha}\delta\theta_\alpha \quad (22)$$

and the range of the indexes are $i = 1...n_o$, $\alpha = n_o + 1...n_1$ and $\mu, \nu = 1...n_1$. We have assumed that there are no a priori limits on the range of the neutrino parameters.

Figure 5 shows evidence ratio as a function of the deviation from the fiducial model, $\{\sum_\nu m_\nu, N_\nu\} = \{0, 3\}$. Again we see that the constraints from the lensing of galaxies and 21 cm put similar constraints on the neutrino parameters. By combining these data sets the constraints are improved by more than a factor of two in each dimension. A combined mass as small as 0.2 eV should be detected, 0.19 eV if N_ν is fixed to 3. Figure 6 shows how these constraints change if the dark energy equation of state is fixed to the cosmological constant value, $\{w_o, w_a\} = \{-1, 0\}$. The constraints drastically improve which again demonstrates the degeneracy between dark energy and massive neutrinos. In this case, a combined mass of 0.09 eV would be detectable.

4 DISCUSSION

If it is assumed that neutrinos are massless, or have too small a mass to be of significance, the dark energy equation of state, $w = p/\rho$, could be underestimated from cosmological constraints. This would be the case even if the data does not allow for a detection of neutrino mass. It is also true that any independent constraint on the neutrino mass would improve future cosmological constraints on dark energy. The KATRIN[8] beta-decay experiment expects to reach a level of 0.2 eV for the electron neutrino mass and thus might have an impact on dark energy constraints. In section 3 it was shown that a neutrino mass as small as $\sum_\nu m_\nu/N_\nu = 0.03$ eV could bias w_o high by $\sim 1\ \sigma$ in future galaxy lensing surveys if it is not accounted for and if it is accounted for the error bars increase by a factor of 3.4 for w_o and 2 for w_a. Lensing of high redshift 21 cm is a way to reduce this degeneracy by adding constraints on the growth of structure at higher redshifts where dark energy is presumed to contribute very little. Type Ia Supernovae surveys and surveys aimed at measuring the baryon acoustic oscillations at $z \sim 1$ will put constraints on dark energy that are based on the luminosity distance redshift relation and so are independent of the growth of structure. It is important that methods based both on structure formation and on luminosity distance are fully realized to avoid systematic errors. The two probes are also necessary to test alternative theories of gravity on large scales which might also provide an explanation for the apparent acceleration of the cosmological expansion.

Acknowledgments

I would like to thank S. White for helpful discussion and criticism. I would also like to thank J. Weller for loaning me his code for calculating the Planck priors on the cosmological parameters.

REFERENCES

Eisenstein, D. J. & Hu, W. 1999, ApJ, 511, 5
Field, G. B. 1959, ApJ, 129, 536
Fogli, G. L., Lisi, E., Marrone, A., & Palazzo, A. 2006, Progress in Particle and Nuclear Physics, 57, 742
Furlanetto, S. R., Oh, S. P., & Briggs, F. H. 2006, Phys.Rep., 433, 181
Hannestad, S. 2005, Physical Review Letters, 95, 221301

[8] www-ik.fzk.de/katrin/

Hannestad, S., Tu, H., & Wong, Y. Y. 2006, Journal of Cosmology and Astro-Particle Physics, 6, 25
Heavens, A. F., Kitching, T. D., & Verde, L. 2007, MNRAS, 380, 1029
Hilbert, S., Metcalf, R. B., & White, S. D. M. 2007, MNRAS, 382, 1494
Jeffreys, H. 1961, Theory of Probability (Oxford University Press)
Kaiser, N. 1987, MNRAS, 227, 1
Kiakotou, A., Elgaroy, O., & Lahav, O. 2007, ArXiv e-prints, 709
Kitching, T. D., Heavens, A. F., Verde, L., Serra, P., & Melchiorri, A. 2008, Phys.Rev.D, 77, 103008
Lesgourgues, J. & Pastor, S. 2006, Phys.Rep., 429, 307
Liddle, A. R., Mukherjee, P., Parkinson, D., & Wang, Y. 2006, Phys.Rev.D, 74, 123506
Lu, T. & Pen, U.-L. 2007, ArXiv e-prints, 710
Madau, P., Meiksin, A., & Rees, M. J. 1997, ApJ, 475, 429
McQuinn, M., Zahn, O., Zaldarriaga, M., Hernquist, L., & Furlanetto, S. R. 2006, ApJ, 653, 815
Metcalf, R. B. & White, S. D. M. 2007a, in preparation
—. 2007b, MNRAS, 381, 447
Morales, M. F. 2005, ApJ, 619, 678
Peacock, J. A. & Dodds, S. J. 1996, MNRAS, 280, L19
Rassat, A., Amara, A., Amendola, L., Castander, F. J., Kitching, T., Kunz, M., Refregier, A., Wang, Y., & Weller, J. 2008, ArXiv e-prints
Saini, T. D., Weller, J., & Bridle, S. L. 2004, MNRAS, 348, 603
Seljak, U., Makarov, A., McDonald, P., Anderson, S. F., Bahcall, N. A., Brinkmann, J., Burles, S., Cen, R., Doi, M., Gunn, J. E., Ivezić, Ž., Kent, S., Loveday, J., Lupton, R. H., Munn, J. A., Nichol, R. C., Ostriker, J. P., Schlegel, D. J., Schneider, D. P., Tegmark, M., Berk, D. E., Weinberg, D. H., & York, D. G. 2005, Phys.Rev.D, 71, 103515
Spergel, D. N., Bean, R., Doré, O., Nolta, M. R., Bennett, C. L., Dunkley, J., Hinshaw, G., Jarosik, N., Komatsu, E., Page, L., Peiris, H. V., Verde, L., Halpern, M., Hill, R. S., Kogut, A., Limon, M., Meyer, S. S., Odegard, N., Tucker, G. S., Weiland, J. L., Wollack, E., & Wright, E. L. 2007, ApJ Sup., 170, 377
Zahn, O. & Zaldarriaga, M. 2006, ApJ, 653, 922
Zaldarriaga, M., Furlanetto, S. R., & Hernquist, L. 2004, ApJ, 608, 622